BOLETIN DE LA SOCIEDAD ESPAÑOLA DE
Cerámica y Vidrio
www.elsevier.es/bsecv

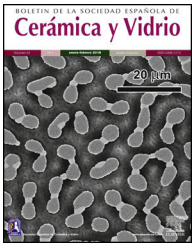

Effect of Cr_2O_3 and Fe_2O_3 doping on the thermal activation of un-polarized PZT charge carriers

*Sakri Adel**, *Bouremel Cherifa*, *Djafri Dhiya Elhak*, *Bouaziz Mounira*

University of Biskra, Box 145 RP, Biskra 07000, Algeria

ARTICLE INFO

Article history:
Received 21 June 2017
Accepted 3 November 2017
Available online 21 November 2017

Keywords:
PZT
Charge carriers
XRD
Resistivity

ABSTRACT

This work suggests a method to evaluate quantitatively the effect of doping oxide on the microstructure phase coexistence, mobility of charge carriers of non-polarized ceramic PZT doping by different amounts of Fe_2O_3 and Cr_2O_3. Besides the analysis of XRD patterns, the electrical properties measurement showed that chromium and iron oxide doping furthers the tetragonal structural phase and disadvantages the rhombohedral structure to a cubic form. Besides, chromium oxide causes more rapidly a mobility of charge carriers of the non-polarized material, compared to iron oxide. Furthermore, the addition of both chromium and iron oxides promotes increase in the size of the tetragonal phase crystal. On the other hand, the rhombohedral phase crystal size increases due to the addition of iron oxide and decreases by doping with chromium oxide.

Efecto de la impurificación de Cr_2O_3 y Fe_2O_3 en la activación térmica de portadores de carga de PZT no polarizado

Palabras clave:
PZT
Portadores de carga
XRD
Resistividad

RESUMEN

Este trabajo sugiere un método para evaluar de manera cuantitativa el efecto del óxido impurificado sobre la coexistencia de fase de la microestructura, la movilidad de los portadores de carga de impurificación de PZT cerámico no polarizado por diferentes cantidades de Fe_2O_3 y Cr_2O_3. Además del análisis de los patrones XRD, la medición de las propiedades eléctricas mostró que la impurificación con óxido de cromo y óxido de hierro fomenta la fase estructural tetragonal y desfavorece a la estructura romboédrica por una forma cúbica. Además, el óxido de cromo genera una movilidad más rápida de los portadores de carga del material no polarizado en comparación con el óxido de hierro. Además, la adición de óxido de cromo y óxido de hierro promueve el aumento de tamaño del cristal de fase tetragonal. Asimismo, el tamaño del cristal de la fase romboédrica aumenta debido a la adición de óxido de hierro y disminuye por la impurificación con óxido de cromo.

* *Corresponding author.*
E-mail address: adelsak@yahoo.fr (S. Adel).
https://doi.org/10.1016/j.bsecv.2017.11.001

Introduction

Lead zirconate titanate (PZT) with perovskite structure is widely studied due to its excellent piezoelectric properties [1,2], and largely used in electronic industry because of its useful piezoelectric properties. Various devices, such as transducers and integrated circuits for microelectronic applications use this type of ceramics [3,4]. The material was intensively investigated since the miscibility of lead titanate and lead zirconate was discovered in the 1950s [5]. Adding different dopants within the basic matrix (PZT) is the way to vary different properties, in order to synthesize new ceramic materials for different applications. For this purpose, many researchers studied the composition of PZT modified by appropriate substitution at sites A and B [6–8], using dopants to improve the electrical and mechanical properties of piezoelectric materials. The properties of PZT samples being highly sensitive to additives, composition and synthesis methods [9].

Electrical conductivity, which directly relates to power losses or charge leakage of piezoelectric devices, is a key physical parameter and appreciably restricts the utilization of several properties of ferroelectrics [10]. An increase in conductivity hinders the determination of the Curie point of known ferroelectrics, using dielectric measurements. Electrical conductivity of ferroelectric ceramics is also essential to the poling efficiency and in turn, the domain configurations [11], which influence the dielectric and piezoelectric properties. For pristine ferroelectric polycrystals, the piezoelectric effect cannot be observable at a macroscopic scale owing to the absence of net polarization. The net polarization, which brings out piezoelectricity, can be developed in polycrystals through the poling process. The poling process depends on the local spontaneous polarization in the unit cells, and can also be reoriented when an adequately strong electric field is applicable, i.e. the

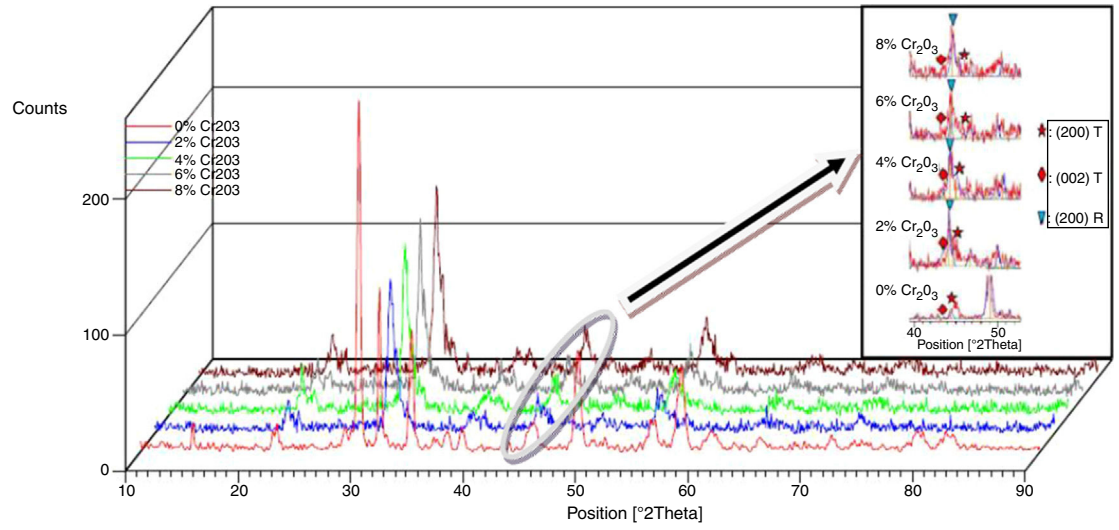

Fig. 1 – XRD pattern of (1 – *x*)PZT-*x* Cr_2O_3 for different composition (*x* = 2%, 4%, 6%, 8%).

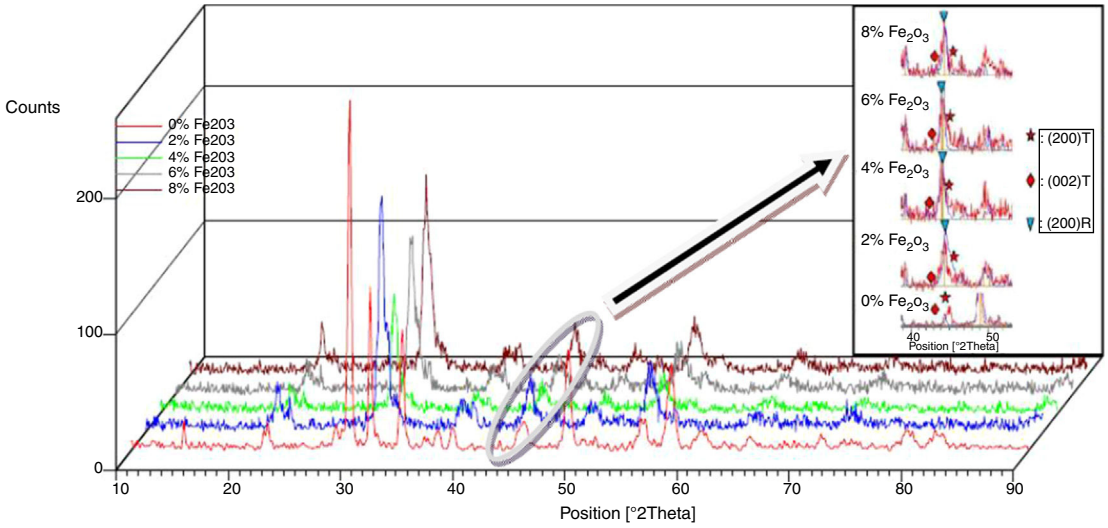

Fig. 2 – XRD pattern of (1 – *x*) PZT-*x* Fe_2O_3 for different composition (*x* = 2%, 4%, 6%, 8%).

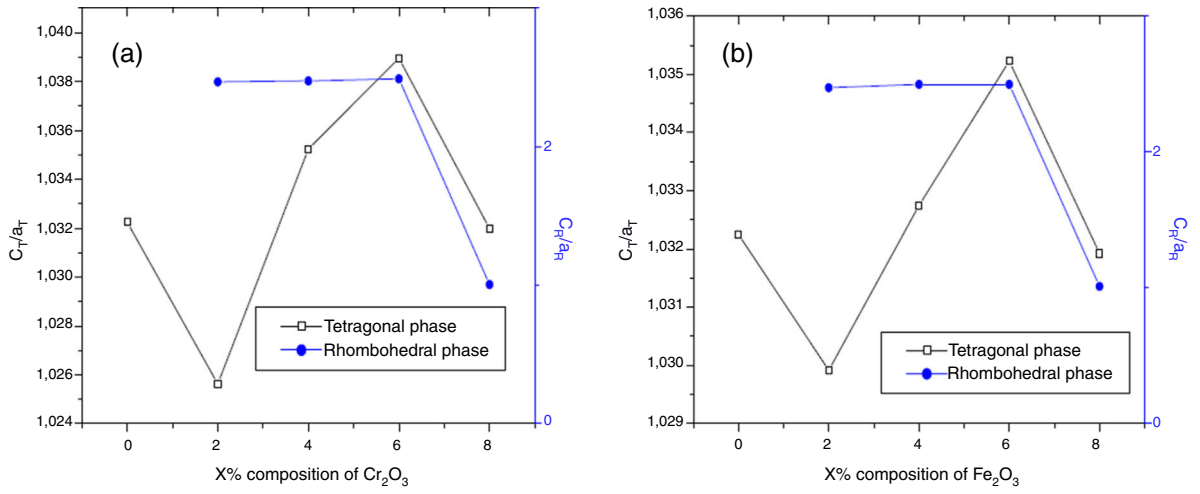

Fig. 3 – (C_T/a_T); (C_R/a_R) as function as composition (a) Cr_2O_3, (b) Fe_2O_3.

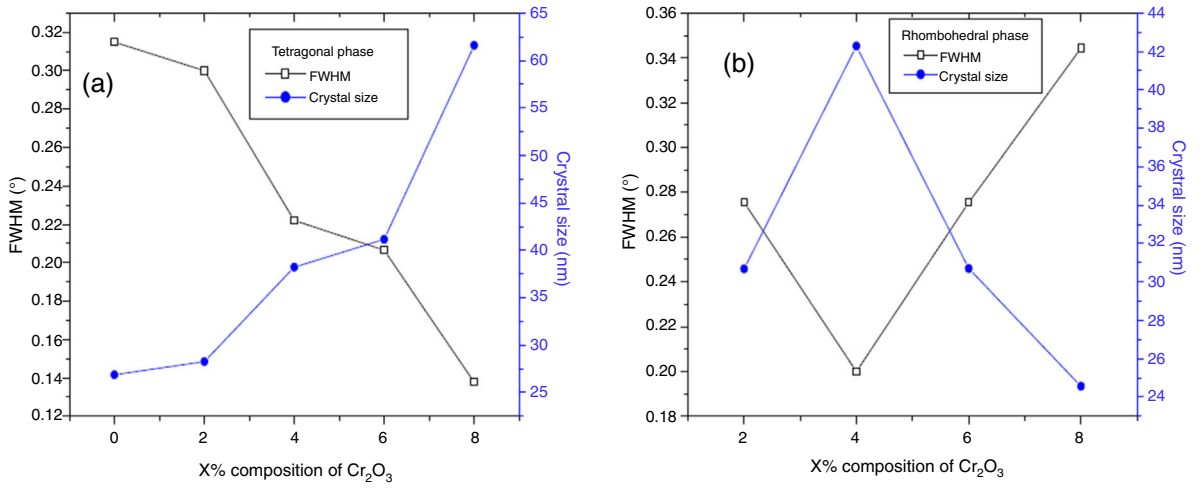

Fig. 4 – FWHM and crystal size as function as Cr_2O_3 composition (a) tetragonal phase, (b) rhombohedral phase.

ferroelectric effect [12]. Reorientation of spontaneous polarization appears in the microstructure, due to either the domain wall motion, or the boundaries separating adjacent domains [13]. Many factors, such as the poling field, poling temperature and poling time, may affect the degree of poling and consequently the piezoelectric properties [14].

A literature survey showed that few groups have reported the temperature-dependent electrical properties of PZT [15]. Basu et al. studied the effect of temperature-dependent electrical properties (dielectric constant, field-induced displacement, electromechanical coupling factor) of PZT wafers made by tape casting. Maiwa et al. [16] investigated the temperature-dependent electrical and electromechanical properties of PZT thin films and concluded that thinner films possess higher Curie temperature. Yimnirun et al. [17] found that the hysteresis area and the remanent polarization of bulk PZT follows the power law temperature-dependent relationship, while the coercivity field scales linearly with temperature. Gubinyi et al. [18] reported the effect of temperature on the electrical properties of PZT bulk. Glaum et al. [19] studied the temperature and field dependent degradation properties of bulk PZT under a unipolar electric field. Chen et al. [20] studied the effect of lead excess on polarization fatigue, and also reported the deterioration of fatigue with increased temperature.

The present work aims to characterize the structural and electrical properties of unpolarized PZT doped with Cr_2O_3 and Fe_2O_3. The microstructure properties, resistivity and conductivity were investigated as a function of the dopant nature, composition and temperature.

Experimental

In the present study, from high purity oxide powders namely, PbO (99.90%), ZrO_2 (99.90%), TiO_2 (99.80%), Cr_2O_3 (99.90%), and Fe_2O_3 (99.90%), samples were prepared by the conventional

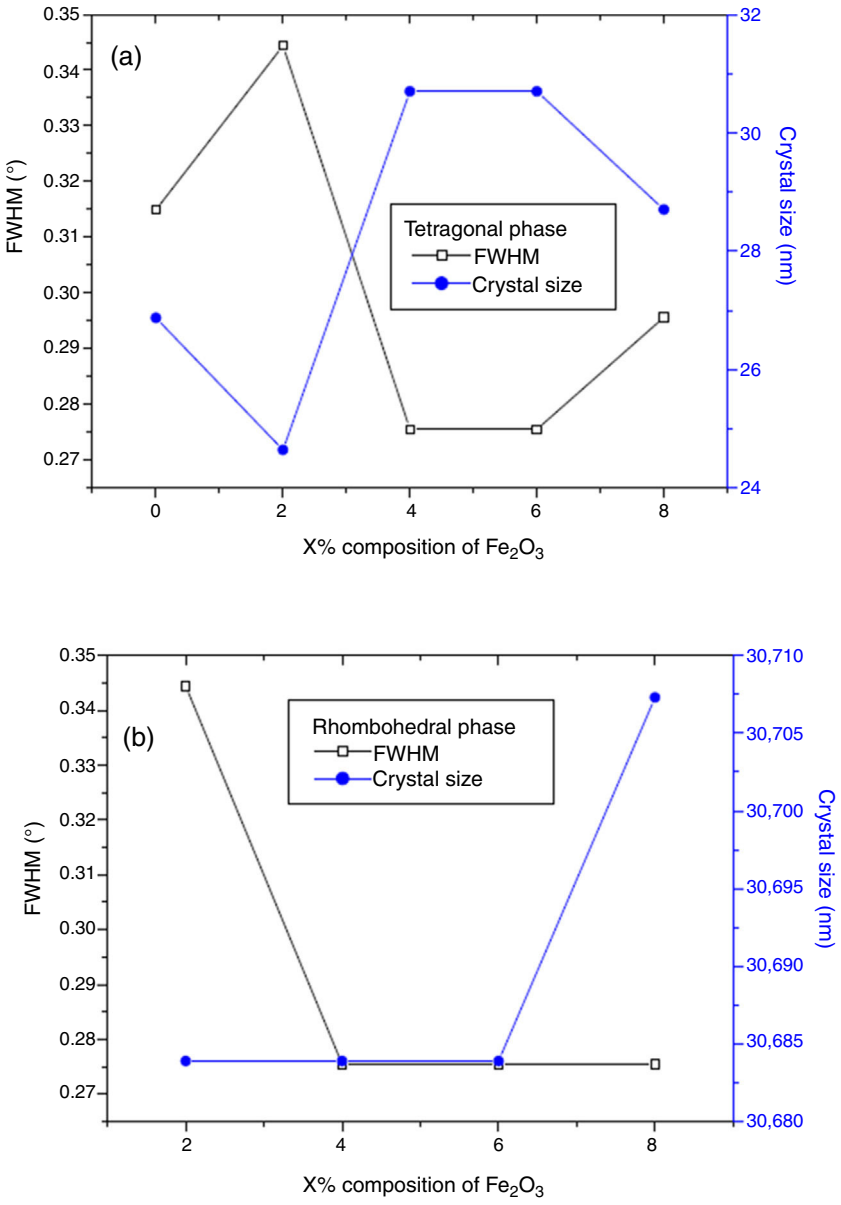

Fig. 5 – FWHM and crystal size as function as Fe_2O_3 composition (a) tetragonal phase, (b) rhombohedral phase.

ceramic process using the formulae $(1-x)$ Pb $(Zr_{0.48}, Ti_{0.52})$ O_3-x Cr_2O_3 and $(1-x)Pb(Zr_{0.48},Ti_{0.52})O_3$-x Fe_2O_3, respectively ($x = 2\%, 4\%, 6\%, 8\%$). The metal stoichiometric amount in the designated $(1-x)$ PZT-x Cr_2O_3 and $(1-x)$ PZT-x Fe_2O_3 composition was mixed for 2 h as grinding media and ethanol as solvent. After milling for 6 h, the resulting slurry was dried in an oven and the powder was calcined in a furnace at 900 °C for 120 min. Then, the calcined powder was ball milled for 6 h to make sure a fine particle size is obtained. After drying, the powder was pressed into disk-like shapes and sintered at 1200 °C in a closed alumina crucible, in a PbO vapor enriched atmosphere, using $PbZrO_3$ powder. An X-ray diffractometer with CuK radiation was used to reveal the phases of the sintered samples. The electrical properties (resistivity and conductivity) were measured using an LCR-meter and programmable oven.

Results and discussion

Microstructure properties

Figs. 1 and 2 show the XRD patterns of $(1-x)$ Pb $(Zr_{0.48}, Ti_{0.52})$ O_3-x Cr_2O_3 and $(1-x)$ Pb $(Zr_{0.48}, Ti_{0.52})$ O_3-x Fe_2O_3 respectively, for various contents (2, 4, 6 and 8%). The tetragonal, tetragonal–rhombohedral phases were identified by analyzing

Table 1 – Phase structure and lattices parameters of $(1-x)PZT\text{-}xCr_2O_3$ and $(1-x)PZT\text{-}xFe_2O_3$.

	X%	Phase	Cell parameters	2θ	FWHM	Intensity %
Doping with Fe_2O_3	0% Fe_2O_3	Tetragonal	$a=b=4.031$ Å; $c=4.161$ Å; $v=67.46$ Å^3	31.3350	0.3149	134.55
				43.4617	0.3149	2.27
				44.4152	0.3149	15.85
	2% Fe_2O_3	Tetragonal	$a=b=4.0216$ Å; $c=4.1419$ Å; $v=66.97$ Å^3	30.98	0.3444	167.26
				43.1744	0.2755	4.87
				45.1955	0.3444	10.08
		Rhombohedral	$a=b=5.772$; $c=14.275$; $v=412.74$ Å^3	30.98	0.3444	167.26
				44.4458	0.3444	31.8
	[2,0]4% Fe_2O_3	Tetragonal	$a=b=4.031$ Å; $c=4.173$ Å; $v=67.63$ Å^3	31.0169	0.4822	110.9
				43.0512	0.2066	5.14
				44.2645	0.2755	23.52
		Rhombohedral	$a=b=5.7588$ Å; $c=14.382$ Å; $v=413.7$ Å^3	31.0169	0.4822	110.9
				44.1245	0.2755	25.52
	[2,0]6% Fe_2O_3	Tetragonal	$a=b=4.031$ Å; $c=4.173$ Å; $v=67.63$ Å^3	31.0169	0.4822	110.9
				43.0512	0.2066	5.14
				44.2645	0.2755	23.52
		Rhombohedral	$a=b=5.7588$ Å; $c=14.382$ Å; $v=413.7$ Å^3	31.0169	0.4822	110.9
				44.1245	0.2755	25.52
	8% Fe_2O_3	Tetragonal	$a=b=4.0129$ Å; $c=4.141$ Å; $v=66.66$ Å^3	31.09	0.4822	131.59
				43.261	0.1	4
				45.14	0.2956	15.5
		Rhombohedral	$a=b=4.082$ Å; $c=4.12$ Å; $v=58.73$ Å^3	31.09	0.4822	131.59
				44.3396	0.2755	32.55
Doping with Cr_2O_3	0% Cr_2O_3	Tetragonal	$a=b=4.031$ Å; $c=4.161$ Å; $v=67.46$ Å^3	31.3350	0.3149	134.55
				43.4617	0.3149	2.27
				44.4152	0.3149	15.85
	2% Cr_2O_3	Tetragonal	$a=b=4.0268$ Å; $c=4.13$ Å; $v=66.98$ Å^3	30.9229	0.4133	105.52
				43.33	0.1	3
				45.08	0.3	16.8
		Rhombohedral	$a=b=5.782$ Å; $c=14.275$ Å; $v=412.9$ Å^3	30.9229	0.4133	105.52
				44.0736	0.2755	23.74
	4% Cr_2O_3	Tetragonal	$a=b=4.001$ Å; $c=4.142$ Å; $v=66.36$ Å^3	30.9563	0.3444	117.6
				43.61	0.01	12.6
				45.1665	0.322	8.81
		Rhombohedral	$a=b=5.761$ Å; $c=14.263$ Å; $v=409.44$ Å^3	30.9563	0.3444	117.6
				44.2334	0.2	23.02
	6% Cr_2O_3	Tetragonal	$a=b=3.9867$ Å; $c=4.142$ Å; $v=65.72$ Å^3	31.0677	0.3444	24.38
				43.2912	0.1755	14.38
				45.7501	0.2066	6.28
		Rhombohedral	$a=b=5.734$ Å; $c=14.282$ Å; $v=406.44$ Å^3	31.0677	0.3444	24.38
				44.2612	0.2755	24.38
	8% Cr_2O_3	Tetragonal	$a=b=4.0117$ Å; $c=4.14$ Å; $v=66.62$ Å^3	31.1642	0.4133	134.1
				43.4338	0.4133	5
				45.2733	0.1378	11.09
		Rhombohedral	$a=b=4.072$ Å; $c=4.094$ Å; $v=58.74$ Å^3	31.1642	0.4133	134.1
				44.3921	0.3444	27.66

the peaks 002 (tetragonal), 200 (tetragonal) and 200 (rhombohedral), in the 2θ range of 43°–47°.

The effect of Cr_2O_3 and Fe_2O_3 content on the microstructure is observed in Figs. 3(a, b), 4(a, b) and 5(a, b). The increasing Cr_2O_3 and Fe_2O_3 content causes a change in the lattice parameters for tetragonal and rhombohedral phases. Generally, the increase in chromium and iron oxide contents favors tetragonality (until $x=0.06$) and disadvantages the rhombohedral form toward a cubic structure.

The increase of Fe_2O_3 content led to an increase in the crystal size for tetragonal and rhombohedral phases gradually, which may be due to the insertion of chrome atoms. However, the increasing Cr_2O_3 amount caused an increase in the crystal size for the tetragonal phase and a decrease in the size

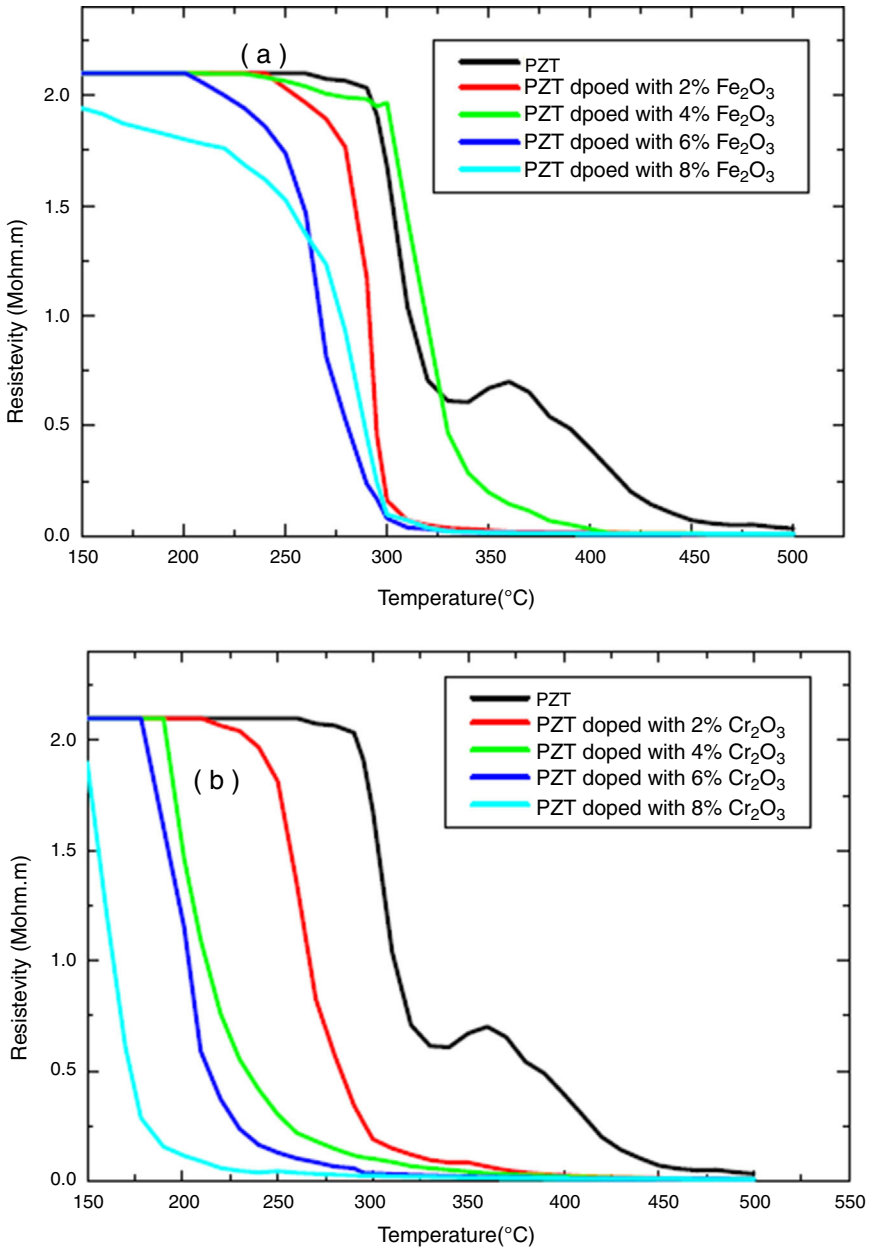

Fig. 6 – Resistivity as function as temperature for different composition (a) Fe_2O_3, (b) Cr_2O_3.

of the rhombohedral phase, This may be assessed to a substitution between the chromium ions with a smaller atomic radius and those of zirconium or titanium with a larger atomic radius. The phase structure and lattice parameters of (1 – x) Pb ($Zr_{0.48}$, $Ti_{0.52}$) O_3-x Cr_2O_3 and (1 – x) Pb ($Zr_{0.48}$, $Ti_{0.52}$) O_3-x Fe_2O_3 samples prepared with various contents are listed in Table 1.

Electrical properties

The electrical properties of (1 – x) PZT-x Fe_2O_3 and (1 – x) PZT-x Cr_2O_3 showed evidence of a phase transformation. Figs. 6(a, b) and 7(a, b) plot the resistivity and conductivity as functions of temperature for various amounts of Cr_2O_3 and Fe_2O_3 doping. As can be seen in these figures, doping with Cr_2O_3 leads to a progressive decrease in the resistivity and increase in the conductivity of samples. This can be assessed to the charge carrier mobility due to the presence of chrome, which therefore makes the sample electrically more conductive. On the other hand, addition of iron oxide results in a decrease in the electrical resistivity of un-polarized samples, in an alternating and non-progressive manner compared to chromium oxide. This may be attributed to the difference in thermal conductivity between chromium (0.937 w/cm k) and iron (0.802 w/cm k) [21]. Consequently, chromium being thermally more conductive, it insures a rapid heat transfer to the charge carriers so that they are thermally excited and mobilized. This trims the un-polarized material electrically less resistant and more conductive, and this is the reverse case of iron.

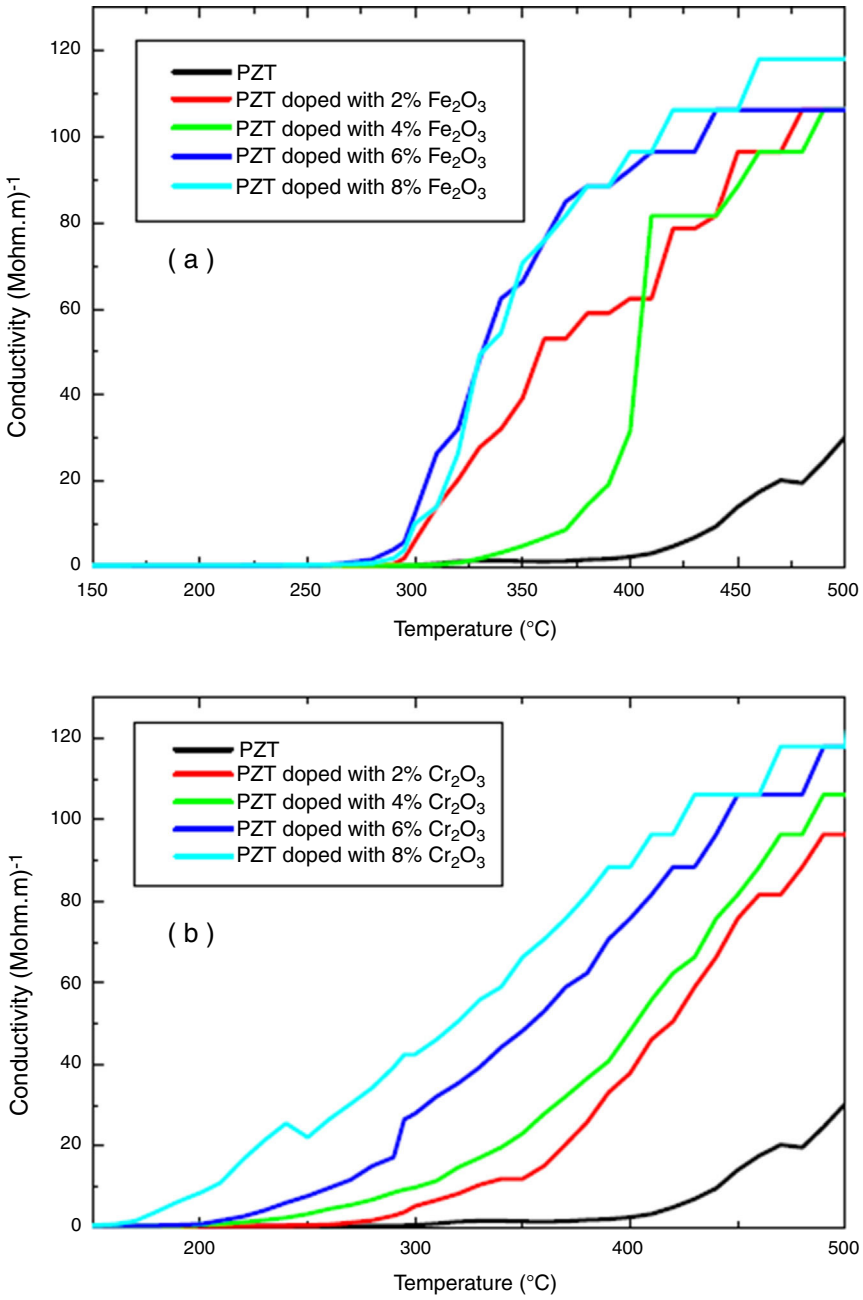

Fig. 7 – Conductivity as function as temperature for different composition (a) Fe_2O_3, (b) Cr_2O_3.

Conclusion

In this paper, X-ray diffraction analysis and electric properties measurement of non-polarized PZT ceramics were implemented to investigate the effect of chrome oxide and iron oxide on the coexistence of rhombohedral tetragonal phases, microstructure and electrical properties. The results show that:

1. The increasing Cr_2O_3 and Fe_2O_3 composition caused a change in the lattice parameters for tetragonal and rhombohedral phases. In general, the increase in the composition of the chromium and iron oxides favors tetragonal moieties (until $x = 0.06$), while it disadvantages the rhombohedral shape toward a cubic structure.
2. The increase of Fe_2O_3 composition results in an increase of the crystal size for tetragonal and rhombohedral phases progressively.
3. Increasing Cr_2O_3 content increases the crystal size of the tetragonal phase and decreases the size of the rhombohedral phase.
4. Addition of Cr_2O_3 decreases progressively the resistivity and increases the conductivity of samples.
5. Addition of Fe_2O_3 causes a decrease in the electrical resistivity of the un-polarized sample in an alternating and non-progressive manner compared to Cr_2O_3 doping.

REFERENCES

[1] Y. Xu, Ferroelectric Materials and Their Applications, North-Holland, Amsterdam and Tokyo, 1991.

[2] C.K. Barlingay, S.K. Dey, Dopant compensation mechanism and leakage current in Pb ($Zr_{0.52}Ti_{0.48}$) O_3 thin films, Thin Solid Films 272 (1) (1996) 112–115.

[3] J. Puustinen, J. Lappalainen, V. Lantto, Effect of microstructure and surface morphology evolution on optical properties of Nd-modified Pb (Zr_xTi_{1-x}) O_3 thin films, Thin Solid Films 516 (18) (2008) 6458–6463.

[4] D. Sun, S.A. Rocks, D. Wang, M.J. Edirisinghe, R.A. Dorey, Novel forming of columnar lead zirconate titanate structures, J. Eur. Ceram. Soc. 28 (16) (2008) 3131–3139.

[5] U. Helbig, Size effect in low grain size neodymium doped PZT ceramics, J. Eur. Ceram. Soc. 27 (7) (2007) 2567–2576.

[6] B. Jaffe, W.R. Cook, H. Jaffe, Piezoelectric Ceramics, Academic Press, New York, 1971.

[7] R. La, S.C. Sharma, R. Dayal, R. La, S.C. Sharma, R. Dayal, Ferroelectrics (1986) 67–93.

[8] R. Rai, S. Sharma, Structural and dielectric properties of Sb-doped PLZT ceramics, Ceram. Int. 30 (7) (2004) 1295–1299.

[9] A. Sakri, A. Boutarfaia, A. Sakri, A. Boutarfaia, Investigation on the structural properties of a new prepared 0.2 PZS-0.8 PLZT ceramics Advanced Materials Research, vol. 856, Trans Tech Publications, 2014, pp. 197–200.

[10] Z. Wrobel, Electrical-conductivity and seebecks coefficient in Pb (Zr_xTi_{1-x}) O_3 solid-solution near the morphotropic phase-boundary 0.46 less-than-or-equal-to × less-than-or-equal-to 0.60, Acta Phys. Pol. A 55 (3) (1979) 267–274.

[11] R. Gerson, Variation in ferroelectric characteristics of lead zirconate titanate ceramics due to minor chemical modifications, J. Appl. Phys. 31 (1) (1960) 188–194.

[12] T. Ogawa, M. Furukawa, T. Tsukada, Poling field dependence of piezoelectric properties and hysteresis loops of polarization versus electric field in alkali niobate ceramics, Jpn. J. Appl. Phys. 48 (9S1) (2009), 09KD07.

[13] M.I. Morozov, H. Kungl, M.J. Hoffmann, Effects of poling over the orthorhombic-tetragonal phase transition temperature in compositionally homogeneous (K, Na) NbO_3-based ceramics, Appl. Phys. Lett. 98 (13) (2011) 132908.

[14] Q. Li, M.H. Zhang, Z.X. Zhu, K. Wang, J.S. Zhou, F.Z. Yao, J.F. Li, Poling engineering of (K, Na) NbO_3-based lead-free piezoceramics with orthorhombic–tetragonal coexisting phases, J. Mater. Chem. C (2017).

[15] T. Basu, S. Sen, A. Seal, A. Sen, Temperature dependent electrical properties of PZT wafer, J. Electron. Mater. 45 (4) (2016) 2252–2257.

[16] H. Maiwa, N. Ichinose, Temperature dependence of the electrical and electromechanical properties of PZT thin films, Ferroelectrics 293 (1) (2003) 89–99.

[17] R. Yimnirun, R. Wongmaneerung, S. Wongsaenmai, A. Ngamjarurojana, S. Ananta, Y. Laosiritaworn, Temperature scaling of dynamic hysteresis in soft lead zirconate titanate bulk ceramic, Appl. Phys. Lett. 90 (11) (2007) 112906.

[18] Z. Gubinyi, C. Batur, A. Sayir, F. Dynys, Electrical properties of PZT piezoelectric ceramic at high temperatures, J. Electroceram. 20 (2) (2008) 95–105.

[19] J. Glaum, T. Granzow, L.A. Schmitt, H.J. Kleebe, J. Rödel, Temperature and driving field dependence of fatigue processes in PZT bulk ceramics, Acta Mater. 59 (15) (2011) 6083–6092.

[20] Z.H. Chen, A.Q. Jiang, Effects of Pb excess and temperature on polarization fatigue in sol-gel derived Pb ($Zr_{0.3}Ti_{0.7}$) O_3 thin films, Ferroelectrics 406 (1) (2010) 83–89.

[21] M.J. Graf, S.K. Yip, J.A. Sauls, D. Rainer, Electronic thermal conductivity and the Wiedemann–Franz law for unconventional superconductors, Phys. Rev. B 53 (22) (1996) 15147.